

and the octet-singlet mixing angle for triplet spin state

$$\theta = 39.5^\circ. \quad (16)$$

With these parameter values the mass of the first radially excited state of the  $\phi(1019)$  is calculated to be 1650 MeV. This nicely accommodates the observed  $\omega(1675)$  [formally called  $\phi(1675)$ ]. The first radially excited state of the  $\omega(784)$  is found to be at 1530 MeV.

The radially excited S-state mesons discussed above are collected in Table II. It should be re-

marked that to obtain an unambiguous assignment of the  $E(1420)$  and  $\omega(1675)$  as radially excited states, one should further analyze the P- and D-state mesons. A consistent analysis of these mesons, however, is found to require the introduction of a tensor potential of the form

$$V_1^T(r) = S_{12} U_1^T(\gamma) e^{-(\beta_1 r)^2}, \quad (17)$$

which we shall not discuss here.<sup>6</sup>

We wish to thank Professor S. F. Tuan for a helpful discussion and some valuable suggestions.

\*Work supported by the National Science Council of the Republic of China.

<sup>1</sup>R. H. Dalitz, in *Proceedings of the Oxford International Conference on Elementary Particles, 1965*, edited by T. Walsh *et al.* (Rutherford High Energy Laboratory, Chilton, Didcot, Berkshire, England, 1966); H. Harari, in *Proceedings of the Fourteenth International Conference on High Energy Physics, Vienna, 1968*, edited by J. Prentki and J. Steinberger (CERN, Geneva, 1968); O. W. Greenberg, in *Proceedings of the Fifth International Conference on Elementary Particles, Lund, 1969*, edited by G. von Dardel (Berlingska Boktryckeriet, Lund, Sweden, 1970); S. Meshkov, in *Proceedings of the International Conference on Duality and Symmetry*

*in Hadron Physics, Tel Aviv, 1971*, edited by E. Gotsman (Weizmann Science Press, Jerusalem, 1971).

<sup>2</sup>I. Butterworth, *Annu. Rev. Nucl. Sci.* **19**, 179 (1969).

<sup>3</sup>Particle Data Group, *Rev. Mod. Phys.* **45**, S1 (1973).

<sup>4</sup>R. Van Royen and V. F. Weisskopf, *Nuovo Cimento* **50A**, 617 (1967); D. K. Katyal and A. N. Mitra, *Phys. Rev. D* **1**, 338 (1970).

<sup>5</sup>R. E. Diebold, in *Proceedings of the XVI International Conference on High Energy Physics, Chicago-Batavia, Ill., 1972*, edited by J. D. Jackson and A. Roberts (NAL, Batavia, Ill., 1973).

<sup>6</sup>See T. Y. Lee and C. T. Chen-Tsai, *Chin. J. Phys.* (to be published).

## Reggeon-calculus approach to high-energy scattering on nuclei

E. S. Lehman and G. A. Winbow

*Daresbury Laboratory, Daresbury, Warrington, Lancashire, WA4 4AD, England*

(Received 8 July 1974)

We apply Reggeon calculus to high-energy scattering on nuclei. Using methods similar to those of Abramovskii, Gribov, and Kancheli, we show that intranuclear cascading is forbidden. The inclusive spectrum is shown to be similar to that on hydrogen targets for rapidities  $\gtrsim \ln(4Rm)$ . We give rough arguments to derive the spectrum for  $y \lesssim y_0$  and show that our results are in qualitative agreement with the data. In weak-coupling theory elastic scattering from nuclei is shown to be factorizable and determined by one-Pomeron exchange. We speculate on the absorption length of the Pomeron in nuclear matter in "weak-coupling" and "strong-coupling" theories. Our model is compared with the "energy flux cascade" model of Gottfried and the Landau model. These have local particle production, in contrast to multiperipheralism, which involves large longitudinal distances. Crucial tests of our model are our predictions that the mean inelasticity of the leading particle is independent of  $A$  and the spectrum  $d\sigma/dy$  is (almost) independent of projectile species.

### I. INTRODUCTION

The reason for studying collisions of very energetic hadrons with nuclei is not what such reactions can teach us about the nucleus (which is probably very little) but rather what we can learn about the dynamics of very-high-energy hadron-

hadron collisions. The usual bubble-chamber or counter experiments detect final-state particles at distances very much larger than the range of the interaction in which they were produced. This means that models that lead to similar predictions for the asymptotic final state will be difficult to distinguish in hadron-hadron experiments, though

their underlying dynamics may be quite different. For a nuclear target the final state of the hadron-hadron system cannot be expected to have completed its development by the time it starts to interact with other nucleons in the target, so we ought to see a dependence of the hadronic final state on the dynamical model chosen.<sup>1</sup>

A simple example shows that there must be such dependence. Consider a model in which the final-state hadrons in a hadron-hadron collision are produced locally, and further let the multiplicity of secondary hadrons produced in a single inelastic collision be  $\langle n \rangle = c \ln s$  when  $s$  is the square of the c.m. energy in the hadron-nucleon system with the final particles produced uniformly distributed in rapidity. This model, which is a reasonable first-order description of the collision, leads to a cascade in the nucleus with each produced particle independently producing secondaries according to its energy as it moves through the nucleus. Several authors have shown that such a model leads to a growth in overall multiplicity with either energy or  $A$ , which is much faster than shown by experiment.

Another reason for studying production with a nuclear target is the availability of ultrahigh-energy data from cosmic-ray projectiles in which the target nucleus is either  $^{14}\text{N}$  or  $^{16}\text{O}$  in an air shower or, predominantly,  $^{107}\text{Ag}$ ,  $^{109}\text{Ag}$  or  $^{79}\text{Br}$ ,  $^{81}\text{Br}$  in emulsion work. Although a determination of the underlying hadron-hadron interaction is not possible by inversion of the hadron-nucleus inelastic scattering, it is definitely possible by such studies to test theories of the interaction between hadrons at high energy.

The most important idea underlying this paper is that in multiperipheral production, particles are created over an extended region of space-time.<sup>2</sup> In particular, many of the particles are created a long time (in the lab frame) before the projectile reaches the target, and they miss the target altogether. In such circumstances, successive collisions in the nucleus do not probe the early development of the particle production process as they would for pointlike production. However, nuclear production is still greatly influenced by the (extended) space-time structure of the production process, as we discuss in later sections.

The simplest multiperipheral process that can occur is when one "comb" is tied onto one nucleon in the target nucleus. This is shown in Fig. 1. If a single multiperipheral process (interacting with only one nucleon in the target) were all that happened, particle production from nuclei would have the *same* multiplicity as from nucleons: The single particle inclusive amplitude and the inelastic cross section would both increase by a factor  $A$ .

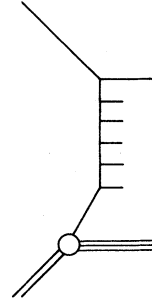


FIG. 1. Simplest multiperipheral process on a nucleus.

Two things can happen to change this. Firstly, more than one multiperipheral chain can be produced in parallel. If each chain is tied onto one nucleon then, apparently, for this diagram with  $A$  chains,  $(d\sigma/dy)_A = A(d\sigma/dy)_H$ . This is illustrated for the deuteron in Fig. 2. Similarly, one of the produced particles in the comb can scatter multiperipherally as shown in Fig. 3. This is a "cascade" process, which would also increase production. Secondly, there can be elastic scattering of the initial or produced particles ("absorption"). This presumably affects particle production as well.

In order to make a proper model of particle production on nuclei we have to take account of these processes. This is clearly the problem of making the model unitary.

In our opinion the strongest candidate for a unitary theory (containing both multiple-comb production and absorption) is Gribov's Reggeon calculus. In this paper we apply this to hadron-nucleus scattering. We take the bare Pomerons to have  $s$ -channel cuts which are simply multiperipheral "combs." The intercept of the bare  $P$  is presumably  $\alpha(0) \neq 1$ .

The bare  $P$  is modified by the self-interaction of the  $P$ . This presumably sets the physical intercept of the  $P$  at  $\alpha(0) = 1$ .<sup>3</sup>

There are two kinds of theories of  $PP$  interaction: the weak-coupling<sup>4</sup> (which has triple-Pomeron

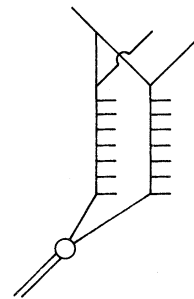


FIG. 2. Double multiperipheral process on deuteron.

zeros, etc.) and the strong-coupling,<sup>5</sup> which is essentially a cut-dominated solution of the Dyson equation for  $P$  self-interaction.

For many considerations we shall use only the bare  $P$  since this is the one whose  $s$ -channel structure is fairly simple. Our main predictions in Secs. III–VI apply to a weak-coupling theory, but we shall point out as we go which of our conclusions would be altered if strong coupling were correct. In Sec. IV we shall see how very-high-energy results for scattering on nuclei might lead to a clear distinction between strong- and weak-coupling solutions.

After this digression on the Pomeron, returning to the question of particle production from nuclei we see that typical diagrams have the same structure as diagrams in a Reggeon-calculus theory of hadron-hadron scattering, assuming, as in Figs. 2 and 3, that each comb or  $P$  is absorbed by only one nucleon. In fact, the  $P$  can be absorbed on more than one nucleon—we shall see the importance of this later. In this way we can apply Reggeon calculus to hadron-nucleus scattering in exactly the same way as in hadron-hadron scattering.

Our technique in the central region is the same as that of Abramovskii, Gribov, and Kancheli<sup>6</sup> (hereafter referred to as AGK). We assume the Reggeon diagrams give a good theory of elastic scattering. We then cut the diagrams by unitarity in the  $s$  channel, thus obtaining strong constraints among production processes. This is the best way we know to try to ensure that production processes satisfy unitarity at high energy. The same results can be obtained by using Mueller-type methods on cut diagrams.

## II. MAIN REGGEON DIAGRAMS

As explained by AGK, the usual assumption that the Reggeon graphs are built by a “softened”  $\phi^3$  theory implies that the only significant  $s$ -channel cuts are those dividing whole Reggeons. Cuts through the sides of multiperipheral ladders are

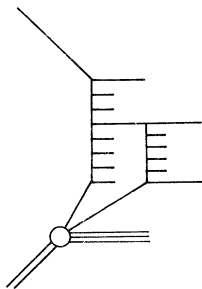


FIG. 3. Cascade process.

negligible.

For example, in Fig. 4, cuts as shown and such that  $\bar{m}^2 \ll \bar{s} \ll s$  are negligible, since by assumption  $q^2$  is cut off at  $|q^2| \lesssim \bar{m}^2$  where  $\bar{m}$  is an unknown model-dependent mass. However, cuts with  $\bar{s} \lesssim \bar{m}^2$  are not forbidden and, for example, play a role in the Amati-Fubini-Stanghellini (AFS) phenomenon. Such cuts lead to production in the fragmentation regions.

In this section we shall quote results that can be proved by a slight extension of the techniques of AGK. Details will be given in a subsequent paper<sup>7</sup> applying these results to hadron-hadron scattering. We discuss the following diagrams.

### A. Impulse diagrams

Here the projectile and target exchange one physical  $P$ . (This is equivalent to a bare  $P$  with arbitrary self-energy insertions.) The analysis of these diagrams is the same as in Ref. 6.

### B. Fan diagrams

These are the simplest diagrams containing a one- $P$  intermediate state in the  $t$  channel, but where there is a multi- $P$  state coupling to several nucleons. Consider for example just the diagram with bare  $P$ 's, the  $\nu$ th-order fan diagram  $\tilde{A}^{(\nu)}$  (see Fig. 5). Let the discontinuity cutting  $\mu$  of the  $\nu$  Reggeons be  $\tilde{F}_\mu^{(\nu)}$ .

One can show,<sup>7</sup> by considering the internal structure of the  $P \rightarrow \nu P$  vertex, that for each  $\mu$  the weight attached to the cut is the same as for an ordinary  $\nu P$  diagram where the top Reggeon is absent. As found by AGK, these weights are

$$i \tilde{F}_0^{(\nu)} = (2 - 2^\nu) \tilde{A}^{(\nu)}, \quad (2.1)$$

$$i \tilde{F}_\mu^{(\nu)} = (-1)^{\nu+\mu+1} 2^\nu \binom{\nu}{\mu} \tilde{A}^{(\nu)}, \quad (2.2)$$

$$\text{Im } \tilde{A}^{(\nu)} = \sum_{\mu=0}^{\nu} \tilde{F}_\mu^{(\nu)} = 2 \tilde{A}^{(\nu)}, \quad (2.3)$$

as expected, since  $\tilde{A}^{(\nu)}$  is pure imaginary. (We neglected the real parts of the  $P$  propagators in

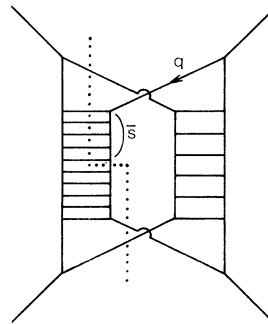


FIG. 4. Discontinuity generally small.

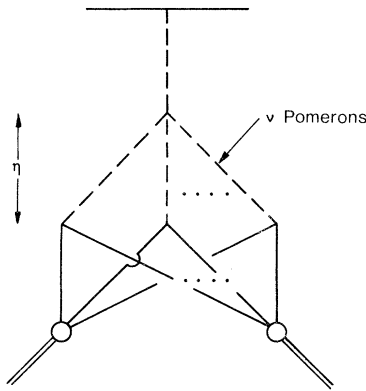


FIG. 5.  $\nu$ th-order fan diagram.

this result—justified at large  $E_L$ . This simplification is not essential.)

Two results follow immediately from this algebra:

(a) The cascade contribution to  $(d\sigma/dy)_A$  is entirely canceled out by absorptive processes.<sup>8</sup> This is clear because at rapidities less than that of the  $P \rightarrow \nu P$  vertex,

$$\sum_{\mu=1}^{\nu} \mu \tilde{F}_{\mu}^{(\nu)} = 0. \tag{2.4}$$

The “cascade” cut is just  $\tilde{F}_{\nu}^{(\nu)}$ .

(b) The higher rapidity production  $y \geq \eta$  coming from the upper  $P$  is uncanceled. It has weight

$$\sigma_{\nu} = \sum_{\mu=0}^{\nu} \tilde{F}_{\mu}^{(\nu)} = 2 \text{Im} \tilde{A}^{(\nu)}. \tag{2.5}$$

We discuss the implications of Eq. (2.5) in the next section.

Higher-order diagrams involving more than one  $P$  “in series” in the  $t$  channel have similar properties to the fan diagrams, but these diagrams are presumably inessential except at ultrahigh energies.

### C. Multi- $P$ exchange

In this class of diagrams there is no one- $P$  intermediate state in the  $t$  channel. Our main result is that in all such diagrams there is no net contribution to  $(d\sigma/dy)_A$  from any process obtained from cutting the original diagram. As an example, the repeated diffractive-multiperipheral excitation shown in Fig. 6 is entirely canceled by other cuts on Fig. 7. This result is discussed in detail in Ref. 7. The essential reason for it is that any  $\nu P$  state contained in a diagram is produced by vertices like the 2 particle  $\rightarrow \nu P$  vertex but containing extra Reggeon interactions. It turns out that the

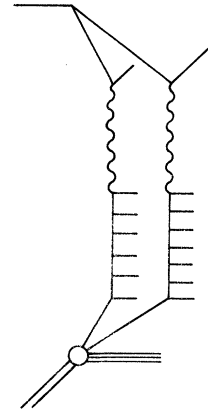


FIG. 6. Example of double diffractive production of high-mass states. The wavy lines can be either bare or physical Pomerons.

Reggeon interactions do not alter the fact that the 2 particle  $\rightarrow \nu P$  vertex is unchanged by  $s$ -channel cutting.<sup>6</sup> Hence the weights attached to the various cuts of the  $\nu P$  state are exactly the same as if all other Reggeons were contracted out.

The conclusion of this section is then that the only multiperipheral production in hadron-nucleus collisions comes from cuts on the single- $P$  intermediate states in the  $t$  channel. At reasonable energies this means that the only multiperipheral production comes from fan diagrams and impulse diagrams.

As a consequence of the remarks made in the introduction to this section, this conclusion only applies to production in the central region, i.e., for  $y_0 < y < y_L - \bar{y}_0$ , where  $y_0, \bar{y}_0$  are model-dependent and  $y_L$  is the lab rapidity of the projectile.)

Finally we note that none of the results of this section depend on  $\alpha(0) = 1$ . If  $\alpha(0)$  is moved to  $< 1$  all the weights of the cuts of the type  $F_{\mu}^{(\nu)}$  ( $\mu \geq 1$ )

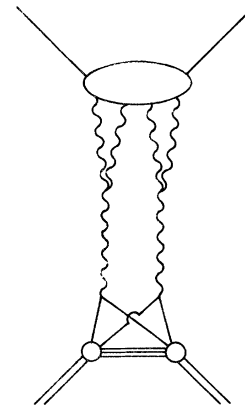


FIG. 7. A diagram containing the production process of Fig. 6 as a discontinuity.

are multiplied by an overall factor; only  $F_0^{(\nu)}$  (and analogous cuts on more complicated diagrams) are changed. In other words, a shift of bare Pomeron intercept alters only the relative weight of the diffraction dissociation contribution. (As a simple example, the reader can check that for double  $f_0$  exchange the cuts  $F_0^{(2)}$ ,  $F_1^{(2)}$ ,  $F_2^{(2)}$  are in the ratios 1: -2: 1, making the overall amplitude real as expected.)

III. CONSEQUENCES OF INFRARED FREEDOM OF THE P

The arguments given in the previous section all apply directly to diagrams involving "bare" Pomerons. In this section we deduce corresponding results for physical Pomerons in the weak-coupling solution. We first consider the triple-P zero.

We showed in Sec. II B that there is uncanceled net production from the second-order fan diagram  $\tilde{A}^{(\nu)}$ . This can be expressed in Mueller's language with physical Pomerons by Fig. 8, which also contains our notation. Let the nuclear vertex be (ignoring correlations)

$$N(K_1^2) = N_0 \binom{A}{2} e^{-2\beta K_1^2}, \tag{3.1}$$

where  $\beta^{1/2}$  is the nuclear radius. In weak-coupling theory the 3P vertex is

$$r(K_1^2) = \lambda \alpha' K_1^2. \tag{3.2}$$

Then Fig. 8 can be written as follows:

$$f(\omega, \bar{\omega}) = g \frac{1}{\bar{\omega}} \psi(p_\perp) \times \frac{1}{\omega} \int \frac{d\omega_1}{2\pi i} \int \frac{dK_1^2 e^{-2\beta K_1^2} \alpha' \lambda K_1^2}{(\omega_1 + \alpha' K_1^2)(\omega_1 - \omega_1 + \alpha' K_1^2)}. \tag{3.3}$$

The integral is

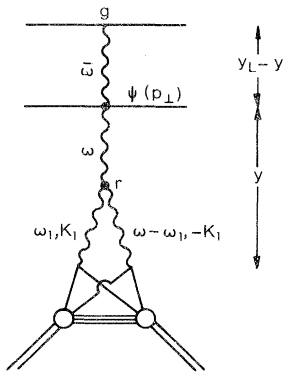


FIG. 8. Mueller diagram to calculate production from a second-order fan diagram.

$$I(\omega) = \lambda \int \frac{dK_1^2 e^{-2\beta K_1^2} (\alpha' K_1^2)}{\omega + 2\alpha' K_1^2}. \tag{3.4}$$

For any reasonable projectile energy  $y_L \ll \beta/\alpha'$ , and since

$$\omega \approx \frac{1}{y} \gg \beta/\alpha' \tag{3.5}$$

we obtain

$$I(\omega) \approx \frac{\lambda \alpha'}{\beta^2 \omega}, \tag{3.6}$$

or

$$\frac{d\sigma}{dy} \approx \frac{g\psi(p_\perp)\lambda\alpha'}{\beta^2} \binom{A}{2} y. \tag{3.7}$$

This is down from a usual Glauber double-scattering term by a factor  $\alpha'/\beta \sim \alpha'/R^2 \sim 10^{-3}$ .

Cardy and White<sup>9</sup> argued on the basis of the Bronzan mechanism<sup>10</sup> for generating the 3P zero that the 2 particle-2P vertex is dominated at  $t=0$  by the fully enhanced term in which the two P's couple to the hadrons through a single P.

The "unenanced" term has a zero at  $t=0$ . In this case the Glauber double-scattering term (2P exchange) must be down by  $O(\alpha'/R^2)$  at high energies when Reggeon calculus becomes applicable.

Cardy has recently extended this argument<sup>11</sup> to claim that P emission from any  $n$ -particle vertex ( $n=0, 1, 2, \dots$ ) is dominated by fully enhanced diagrams in the P lines. In this case, the following statements hold:

- (i) The whole Glauber multiple-scattering (repeated exchange of P) series is down by  $O(\alpha'/R^2)$ .
- (ii) All fan diagrams are similarly reduced except for ridiculously high energies  $y \sim \beta/\alpha'$ . This corresponds to  $E_L \sim 10^{100}$  GeV, which is the energy required for a Regge radius to be comparable with a nuclear radius.
- (iii) Particle-nucleus scattering is dominated by diagrams of the type of Fig. 9 at very high energy

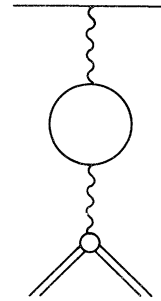


FIG. 9. Dominant class of diagram in weak-coupling theory at very high energy. The blob contains arbitrary Pomeron graphs.

and is therefore factorizable. Particle-nucleus and particle-particle elastic scattering are then determined by one- $P$  exchange obtained by summing all diagrams of type Fig. 9.

In this case production throughout the whole central region will be the same for any projectile and target. The normalization of  $d\sigma/dy$  depends on the penetration depth of the  $P$  in nuclear matter as discussed in Sec. V;  $d\sigma/dy$  is, of course, determined by inserting a throughgoing line corresponding to the observed secondary in any 1- $P$  state of Fig. 9. It will in general be a flat distribution in  $y$ , corrected by inverse powers of  $y$ .

#### IV. PROJECTILE AND TARGET FRAGMENTATION

The analysis of Secs. II and III is not applicable in the fragmentation regions. This is because cuts out of the sides of Reggeons are allowable there.

Consider first the projectile fragmentation region. The same arguments as used in Sec. III imply that Fig. 10 is dominated by the corresponding fully enhanced diagram, and hence is proportional to  $y_L \alpha' / \beta^2$ , which is negligible for any reasonable  $E_L$ .

Hence in a Mueller type of analysis the  $a\bar{c} - a\bar{c}$  amplitude emits only one Pomeron. It immediately follows (recalling Secs. II and III) that the spectrum  $(1/\sigma_{\text{inel}})d\sigma/dy$  must be the same for any target outside the target fragmentation region. We shall see in Sec. VI that current data are consistent with this picture at upwards of 200 GeV.

Although arguments using Reggeon calculus are not applicable in the nuclear fragmentation region, we can still apply multiperipheral notions. As is well known, in the multiperipheral model particles are produced in a region of  $z$  and  $t$  (in the lab frame) of length  $\approx E_L / mm_\pi$  and (which is less important for our present discussion) over impact parameters  $b \approx 2[\alpha' \ln(s/s_0)]^{1/2}$ . It also follows from this that the  $P$  can be regarded as a collective excitation of hadronic matter extended over a region of space-time of the same dimensions. It is precisely for this reason that the classical cascading picture has broken down in the central region.

The rapidity bounding the target fragmentation region can now be determined. Look first in the nuclear rest frame. What happens in the central region is that due to time dilation the multiperipheral fluctuations ("partons") of the projectile (in the lab frame) persist over distances  $\gg 2R$ , the nuclear diameter, and hence can interact with the whole nucleus at once.

However, partons slow in the lab frame cannot persist across a nuclear diameter. The dividing line is at  $E_0 / \bar{m} m_{\pi\perp} \approx 2R$ ; that is,

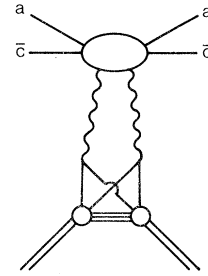


FIG. 10. A rescattering diagram contributing to production in the projectile fragmentation region.

$$y_0 = \ln \left( \frac{2E_0}{m_{\pi\perp}} \right) = \ln(4Rm), \quad (4.1)$$

independent of the transverse mass,  $m_{\pi\perp} = (p_\perp^2 + m_\pi^2)^{1/2}$ , of the  $\pi$ . Above this rapidity the production is over an extended region of space-time in the lab frame. Below this rapidity production becomes essentially local and sequential as the projectile passes through the nucleus.

Alternatively we can look in an arbitrary frame of reference, of rapidity  $y$  relative to the nucleus. Recall that in multiperipheral interactions, in every frame of reference only the slow partons interact. If  $y > y_0$ , then the nucleus is Lorentz-contracted to a thickness  $\approx 1/m_\pi$ , and slow partons which are fragments of any nucleon along a trajectory at fixed  $\bar{b}$  can be found within  $1/m_\pi$  of any slow parton which is a fragment of the projectile. If  $y < y_0$ , this is no longer possible because the parton fragments of nucleons at opposite ends of a nuclear diameter do not live long enough to both reach the neighborhood  $\approx 1/m_\pi$  within a parton fragment of the projectile. Hence the nucleus scatters a parton of rapidity  $y \lesssim y_0$  sequentially from target nucleons.

In the multiperipheral model hadrons do not contract to arbitrarily thin "plates" at high energies. They never become thinner than  $\approx 1/m_\pi$  as measured by another hadron.

We conclude that because of the extended space-time structure of the production mechanism (and hence of the  $P$ ) projectiles with energy exceeding about  $2R \bar{m} m_\pi$  interact with a nucleus  $A$  in the same way. The intermediate-state particles with energy  $> 2R \bar{m} m_\pi$  see a transparent nucleus. Particles with energies less than this have only short lifetimes as virtual states in the lab frame; hence they must be considered as nuclear fragments rather than virtual fluctuations of the projectile.

We show in Fig. 11 a qualitative sketch of  $(1/\sigma_{\text{inel}})(d\sigma/dy)$  according to the discussion in this and the preceding section. The situation will be the same in strong-coupling theory provided (i) fully enhanced diagrams dominate, and (ii) nuclear

rescattering is negligible.

Condition (i) is apparently fulfilled,<sup>12</sup> at least asymptotically, but we do not know if (ii) is true in strong-coupling theory, though it will be true if the  $P$  is absorbed only on the outside of the nucleus. Our discussion of the target fragmentation region is independent of the nature of  $PP$  interaction.

The absolute normalization of  $\sigma$  and  $d\sigma/dy$  depends on nuclear effects as discussed in the next section.

## V. EFFECTS OF THE OPACITY OF NUCLEAR MATTER

### A. Multiple-scattering theory

It has been known for a long time<sup>13</sup> that in a medium or heavy nucleus, multiple scattering screens the interior nucleons from a projectile ( $p$ ). Suppose, for example, a projectile of lab energy  $E_L$  has a mean free path in nuclear matter of  $\lambda(E_L)$ . The unscreened nucleons lie within a distance  $\lambda$  in the projectile direction from the surface of the nucleus. Hence

$$\sigma_T \approx \left( \frac{R^2 \lambda}{R^3} \right) A \sigma, \quad (5.1)$$

where  $R$  is the radius of a nucleus  $A$  and  $\sigma$  is the  $pN$  cross section.

Using  $\lambda^{-1} = \rho_0 \sigma$ ,  $\rho_0$  being the number density of nuclear matter, we have the usual result that a medium or heavy nucleus has a cross section

$$\sigma_T \approx R^2 \propto A^{2/3}. \quad (5.2)$$

This is well observed in the range  $1 < E_L < 70$  GeV.<sup>14,15</sup> More formally, in the optical picture of scattering,<sup>13</sup>

$$\sigma_T = 2 \int d^2b (1 - e^{-1/2 \sigma T(b)}), \quad (5.3)$$

where  $T(b)$  is the optical thickness of the nucleus

$$T(b) = \int_{-\infty}^{\infty} \rho(z^2 + b^2) dz. \quad (5.4)$$

Noting then that Eq. (5.3) is independent of  $\sigma$  (to leading order in  $A$ ), we see that a rise in the  $pN$  cross section will have little effect on  $\sigma_T$ .

### B. Effects due to the structure of the bare $P$

The above discussion takes no account of the mechanism of  $pN$  scattering except that it is mainly absorptive. Now for unattainably high energies ( $4\alpha' \ln s \gtrsim R^2$ ) the optical argument must break down.<sup>16</sup> The inverse powers of  $\ln s$  in the terms of the multiple-scattering series eliminate the rescattering terms and the nucleus becomes transparent.

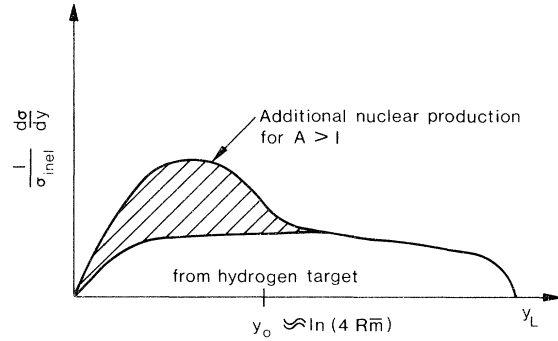


FIG. 11. Production from a nucleus at high energy.

Gribov has argued that due to the multiperipheral structure of particle production (and hence of the  $P$ ) one will still have  $\sigma_T \propto A^{2/3}$  at  $E_L \rightarrow \infty$  even if

$$E_L \gg \exp\left(\frac{R^2}{\alpha'}\right). \quad (5.5)$$

The reason for this is that elastic scattering from a nucleus looks, in the multiperipheral picture, from the point of view of the nucleus, like elastic scattering of the last link in the multiperipheral chain from the nucleus (see Fig. 12). Such a link has some mean free path  $\bar{\lambda}$  in nuclear matter. Hence although single- $P$  exchange dominates when Eq. (5.5) is satisfied, only nucleons within  $\bar{\lambda}$  of the surface can contribute and hence we have

$$\sigma_T \approx \frac{R^2 \bar{\lambda}}{R^3} A \sigma, \quad (5.6)$$

and so again  $\sigma_T \propto A^{2/3}$ .

Clearly  $\bar{\lambda}$  is highly model-dependent, but we might guess  $\bar{\lambda} \sim (\rho_0 \bar{\sigma})^{-1}$  where  $\bar{\sigma}$  is, say, the mean  $pN$  cross section over the range  $E_L = 0 \rightarrow 1$  GeV. This would be smaller than  $\lambda$ . Hence if other effects are negligible the total nuclear cross sections will fall firstly in the region (5.5) but also at much lower energies: those when particle production is dominated by a central plateau (when presumably the  $P$  is mostly built up multiperipherally).

At such energies multiple scattering from nuclei will be suppressed, just because of this "skin

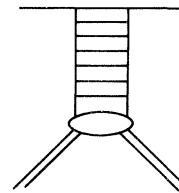


FIG. 12. Exchange of a "bare" Pomeron contains the scattering of a link on the nucleus.

effect" of the nucleus. This might be detected by studying the dip-bump structure of elastic differential cross sections on nuclei. (We mean "elastic" in the sense of the final states being the projectile plus  $A$  nucleons in any arrangement.) The "skin effect" can be expressed in a different way by saying that because the  $P$  is an extended structure in space-time, it can couple to more than one nucleon in the target nucleus.

We can summarize all this by saying that at high energies a new length scale appears in the interaction of hadrons with nuclei. This is  $\bar{\lambda}$ , the absorption length of the  $P$  in nuclear matter. It is only a guess that  $\bar{\lambda} \approx 1-2$  fm.

We now sketch some arguments to show that the above discussion can be a serious oversimplification at ultrahigh energies. In fact the  $A$  dependence of  $\sigma_T$  may depend on the  $PP$  interaction.

### C. Absorption length of the $P$ in a nucleus in strong- and weak-coupling theories

We consider firstly the expansion of the elastic amplitude in terms of bare  $P$ 's and their interactions, assuming  $\alpha(0)$  is close to unity. At the same time, one has the expansion in terms of the physical  $P$  whose intercept is 1. If  $|1-\alpha(0)| \ll 1$ , for a substantial range of  $s$  the physical  $P$  will be quite close in  $s$ -channel structure to the multi-peripheral state and Gribov's argument will apply whether we have weak- or strong-coupling theories.

For weak coupling the theory is always multi-peripheral in the sense that although we have at large  $s$  many combs in series and in parallel (giving the fluctuations discussed by AGK), still the average momentum transfer in the production process stays finite and Gribov's argument is applicable.

However, in the case of strong-coupling theory an entirely different situation is possible. In the strong-coupling situation, the physical  $P$  is a long way from a pole and hence does not have a multi-peripheral  $s$ -channel structure. The mean multiplicity in  $NN$  collisions can increase faster than  $\ln s$ , say, as  $(\ln s)^{1+\delta}$  ( $\delta > 0$ ). In such a case the momentum transfers between adjacent rapidity-ordered secondary hadrons will not be finite as  $s \rightarrow \infty$ . One commonly assumes that the cross section of a heavy off-shell hadron on any hadron is small. Hence it is quite possible that the nucleus can be transparent and  $\sigma_T \propto A$ .

Unfortunately we cannot go so far as to say that the  $A$  dependence of  $\sigma_T$  tells us whether we have weakly or strongly coupled  $P$ 's. In fact  $\delta$  can be close to zero (say,  $\frac{1}{6}$ ).<sup>12,17</sup> Then the nucleus only becomes transparent at ridiculously high energy.

Secondly, we do not know the form of  $\mathcal{L}_{\text{int}}(P)$  and strong-coupling results depend on this.<sup>12,17,18</sup>

All we can say is that if  $\sigma_T$  eventually increases like  $A^1$ , weak coupling is probably ruled out.  $\sigma_T \propto A^{2/3}$  is compatible with either weak coupling or some forms of strong coupling.

We need data on  $\sigma_T$  and  $d\sigma/dt$  for nuclei up to the highest energies possible.

## VI. EXPERIMENT

In Secs. II-IV we saw that the secondary spectrum  $d\sigma/dy$  is divided into two regions—the "nuclear" part at  $y \leq y_0 = \ln(4R\bar{m})$  and the "hadronic" part at  $y \geq y_0$ . In Sec. V we saw how the  $P$  can be absorbed in nuclear matter and how this would qualitatively affect the cross section.

In this section we work out the experimental consequences of the weak-coupling theory, in which  $\sigma_{\text{inel}}$  and  $d\sigma/dy$  are both dominated by the exchange of a physical  $P$  complete with its self-interaction terms (see Fig. 9). This theory only becomes exact at high energies, when multiple-scattering effects have gone away. These could be significant at accelerator energies, but as we shall see below, they are unnecessary for present data at FNAL energies.

The following calculations are approximate only, and simply meant to show that our theoretical arguments produce multiplicities reasonably in accord with present data. In particular, we treated production as essentially only dependent on  $y$  at energies above 200 GeV and we oversimplified the discussion of the transition region  $y \sim y_0$ . We feel such a rough approach is justified by the rough character of the data above 200 GeV, and by the fact that total mean multiplicity data are clearly not a strong test of the validity of our assumptions. (As we mention at the end of this section, the forward proton spectrum is a much stronger test for the Reggeon calculus approach to pass.) We define

$$n_b(A, y) \equiv \frac{1}{\sigma_{\text{inel}}} \left( \frac{d\sigma}{dy} \right)_A \quad (6.1)$$

for a projectile  $b$  incident on a nucleus  $A$ . (We have seen that for  $y \geq y_0$  this is independent of  $A$ .)

In Sec. IV we argued that production in the target fragmentation region ( $y < y_0$ ) can be regarded as coming from successive collisions on nucleons of a "parton" of rapidity  $y_0$ . Then, for  $y \leq y_0$ ,

$$n_b(A, y) = \bar{N} n_{\text{parton}}(1, y), \quad (6.2)$$

where  $\bar{N}$  is the mean number of collisions of the parton in crossing the nucleus. (The effect of possible cascades is small because  $y_0$  is not large.) Experimentally  $n(1, E_L)$  is independent of



the projectile, so what model we take for the parton makes little difference for this. We can think of it as some kind of average meson and put  $\pi N$  cross sections in our formulas.

Integrating (6.1) and (6.2) we obtain

$$\bar{n}_b(A, E_L) = \bar{n}_b(1, E_L) + (\bar{N}-1)\bar{n}_{\text{parton}}(1, E_0), \quad (6.3)$$

where the  $\bar{n}$ 's are total mean multiplicities. To derive (6.3) we assumed scaling which is reasonable as we are concentrating on energies rather higher than the top Serpukhov energy. Our approach is only sensible if  $y_L \gg y_0$  and for an emulsion target  $E_0 \approx 50$  GeV.

To evaluate the right-hand side of Eq. (6.3) we use the empirical formula, valid for  $E_L \gtrsim 50$  GeV (see Ref. 19),

$$\bar{n}_p(1, E_L) = 1.65 \ln E_L - 0.8. \quad (6.4)$$

(Our results in Fig. 13 are not very sensitive to this parametrization.)

For  $\bar{n}_{\text{parton}}(1, E_0) [\equiv n'(y_0)]$  we used

$$n'(y_0) = \frac{1}{2} \bar{n}_p(1, E_0'), \quad (6.5)$$

such that

$$2y_0 = \ln(2E_0'/m). \quad (6.6)$$

We took the nucleus as a uniform sphere of density  $\rho = 0.17 \text{ fm}^{-3}$  and thus of radius

$$R = R_0 A^{1/3}, \quad (6.7)$$

where  $R_0 = 1.1 \text{ fm}$ .

With this geometry one can easily check that, using

$$\lambda(\text{parton-nucleon}) = (\rho \sigma_{\pi N})^{-1}, \quad (6.8)$$

we have

$$\bar{N} = \sigma_{\pi N} A^{1/3} / \pi R_0^2, \quad (6.9)$$

where  $\pi R_0^2 = 39 \text{ mb}$  and we took  $\sigma_{\pi N} = 20 \text{ mb}$ .

Finally we define a parameter

$$R_b(A, y_L) \equiv \frac{\bar{n}_b(A, y_L)}{\bar{n}_b(1, y_L)} \quad (6.10)$$

and obtain

$$R_b(A, y_L) = 1 + \frac{n'(y_0)}{\bar{n}_b(1, y_L)} \left( \frac{\sigma_{\pi N} A^{1/3}}{\pi R_0^2} - 1 \right). \quad (6.11)$$

Note that  $\bar{n}_b(1, y_L)$  contains all the dependence on the projectile species  $b$ , and this is known to be experimentally very weak.<sup>20</sup>

For the present we ignore the complications of the nature of the secondary spectrum near  $y = y_0$ , of (small) correction terms, and of the detail of  $PP$  interaction and just compare our results (6.1), (6.2), and (6.11) with data.

With essentially no free parameters, we shall

be able to account qualitatively for the following data.<sup>21</sup>

(1) In and near the projectile fragmentation region the  $\ln \tan \theta_L$  plots for H, C, and emulsion (Em) targets are about the same.

(2) The mean inelasticity of the leading particle is  $\langle K \rangle \approx 0.5$  independent of  $E_L$  or  $N_L$ .

(3) In the backward hemisphere there is additional production on C and Em. Its amount can be expressed by the parameters

$$R_C \equiv R_p(12, y_L) \approx 1.2$$

and

$$R_{\text{Em}} \equiv R_p(67, y_L) \approx 1.7,$$

roughly independent of  $y_L$ . ( $\bar{A} \approx 67$  for emulsion.)

(4)  $d\sigma/dy$  is roughly forward-backward symmetric for  $N_h = 0$  or 1 (and may be even slightly forward asymmetric). For larger  $N_h$  it becomes backward asymmetric.<sup>22</sup>

(5)  $\bar{n}_p(67, E_L) \propto N_h$ .

(6) To judge from the relative numbers of events with different  $N_h$ , the nuclear response is about the same at  $E_L = 25$  GeV as at  $E_L = 200$  GeV.

Taking these points in turn, we first recall Eq. (6.1).

Agreement with points (1) and (2) is immediate. We have plotted in Fig. 13 our predictions of  $R_p(A, y_L)$  for several  $A$  (and for comparison the predictions of the energy flux model of Gottfried<sup>1</sup>). The agreement is reasonable. We draw attention to a possible drop in  $R_{\text{Em}}$  between 69 GeV/c and 200 GeV/c.<sup>23</sup> Such an effect might be expected as  $E_L$  increases to exceed  $E_0$  ( $\approx 50$  GeV for emulsion).

On point (4), events with  $N_h = 0$  or 1 mostly correspond to only one nucleon struck in the target. Hence production should be about the same in  $\ln \tan \theta_L$  distribution as on H.

The number of nucleons struck in a particular event is  $\bar{N}$ , each nucleon receiving a randomly directed momentum presumably of order 0.4 GeV/c. Just how many nucleons are subsequently ejected clearly depends on nuclear physics, but it should finally be proportional to  $\bar{N}$  which gives result (5) above.

We can easily estimate that the nuclear response will settle down as  $y_L$  passes  $y_0$ . For emulsion this occurs at around  $E_L = 50$  GeV—perfectly consistent with point (6).

We have seen that the shape of the spectrum in the near forward region is the same for any nuclear target. This leads immediately to our most striking prediction.  $\langle K \rangle$  is independent of  $A$ . This prediction should give a clear test of any type of model of the present kind versus the "hadronic matter" type of models discussed in Sec. VII.

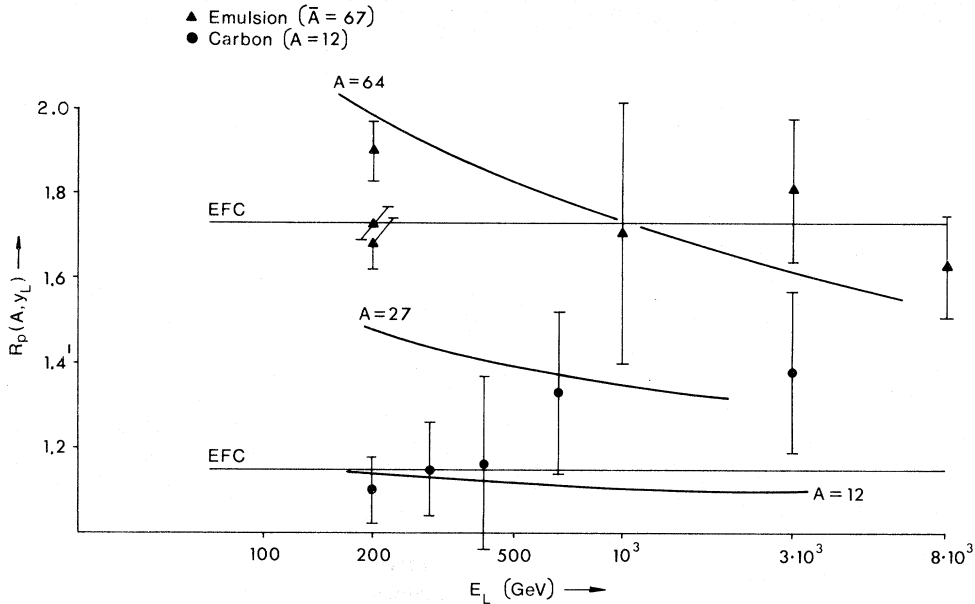


FIG. 13. Predictions for charged multiplicities for several  $A$  at various energies. Horizontal lines are predictions of the energy flux cascade model. Sloping lines are predictions of the present model.

#### VII. COMMENTS ON THE LANDAU<sup>24</sup> AND GOTTFRIED<sup>1</sup> MODELS

These models both involve the notion of a continuum state of "hadronic matter."

The basic motivation is as follows. Consider two relativistic particles produced from a nucleon  $N_1$ . They will in general hit a second nucleon  $N_2$  after traveling a distance  $\approx 2-3$  fm, the mean free path of hadrons in nuclear matter. It is easy to check that when they reach  $N_2$  their "centers" will have separated a distance much less than one fermi. Hence it is argued that one should not consider them as separate particles (as in a classical cascade model). Presumably, hadronic matter confined in a box of size  $\approx 1$  fm does not have a definite number of particles because of strong creation and absorption of virtual particles.<sup>25</sup> In this view one is only entitled to count the number of produced particles after the produced hadronic matter has left the nucleus.

These arguments only carry weight if one believes that the secondaries are produced in a region of dimensions  $1/m_\pi$  in the lab frame.

The space-time properties of the multiperipheral model are completely different. As is well known,<sup>2</sup> from the point of view of the target, the secondary production looks like multiperipheral splitting of the projectile. The secondaries are produced in a tube of length  $O(E_L/m)$  and radius  $O(\ln E_L/m)^{1/2}$ , most of them a long time before the projectile reaches the target (as seen by the target). It is

clear then that multiperipheral production in principle evades the arguments for regarding the process as one involving blobs of hadronic matter which eventually fragment into hadrons.

A point against the Landau and Gottfried models is that they involve extra hypotheses, in one case about thermodynamics being applicable to hadronic matter, and in the other case about "slicing" the hadronic matter into equivalent hadrons. Such hypotheses are very hard to derive from deeper principles and may therefore be regarded as somewhat arbitrary. By contrast no such hypotheses are necessary for the application of the Reggeon-calculus-diagrammatic point of view, although obviously we have to grapple with the problem of unitarity, which is what all those complicated Reggeon graphs are about.

It is well known also that models referring to "hadronic matter" have difficulty in accounting for the leading particle effect.

We think that a decision between our point of view and that of Landau and Gottfried can definitely be made on the basis of our prediction in Sec. V that the inelasticity of the leading particle is independent of  $A$ .

We also predicted that  $R_b(A, y_L)$  is largely independent of  $b$ . In the energy flux model one would presumably expect  $R_b$  to be appreciably greater than  $R_\pi$  for both light and heavy nuclei since  $\sigma_{\text{inel}}(pN) \approx \frac{3}{2} \sigma_{\text{inel}}(\pi N)$ . We note that at 60 GeV/c, where the energy flux model should be applicable, this seems not to be the case.<sup>26</sup>

## VIII. COMMENTS ON A PAPER OF KANCHELI

Kancheli has recently applied Reggeon calculus to the question of high-energy inelastic scattering on nuclei.<sup>27</sup> He concludes (without detailed discussion) that Reggeon calculus forbids intranuclear cascading in the central region. (Reference 6 contains an error relevant to this point, which we correct in our accompanying paper.<sup>7</sup>) He also has given intuitive arguments quite similar to our own arguments on the target fragmentation region. He ascribes a prominent role to the fan diagrams (see Fig. 14) and concludes (for unstated reasons) that  $l \approx 1$  for  $y \sim \text{finite}$  and  $l = A^{1/3}$  for  $y \approx y_L$ . On this basis one obtains

$$\frac{d\sigma}{dy} \propto A^1 \text{ for } y \approx 1, \quad (8.1)$$

$$\frac{d\sigma}{dy} \propto A^{2/3} \text{ for } y \approx y_L. \quad (8.2)$$

The reason that  $l=1$  dominates at smaller  $y$  is presumably that given in Sec. III—infrared freedom of the Pomeron reduces multiple scattering [Eq. (3.7)]. That  $l \sim A^{1/3}$  dominates for  $y \sim y_L$  follows upon neglecting the  $l$  dependence of the central  $P \rightarrow lP$  vertex in comparison with the alternating sign  $(-1)^l$ , and working at such large  $y_L$  that  $y \sim \beta/\alpha'$  is allowed. For practical purposes this is unattainable, and  $l \sim 1$  always (see Sec. III above).

Thus Kancheli is predicting that at accelerator energies  $d\sigma/dy \propto A$  for  $y_0 < y < y_L$ . In our opinion this should be corrected because the  $P$  is only absorbed on the surface of the nucleus in a weak-coupling theory.

Kancheli also presents some interesting speculations on nucleus-nucleus scattering and particle-nucleus scattering at ultrahigh  $y_L$ .

## IX. SUMMARY AND CONCLUSIONS

Our main conclusions are the following:

- (1) There is no cascading except possibly in the target fragmentation region, where it would be fairly unimportant because not much energy is available there.
- (2) The spectrum  $d\sigma/dy$  for  $y \lesssim \ln(4R\bar{m})$  is the same in angular distribution (neglecting rescattering effects) but  $\approx \sigma_{\pi N} A^{1/3} / \pi R_0^2$  greater than on hydrogen.

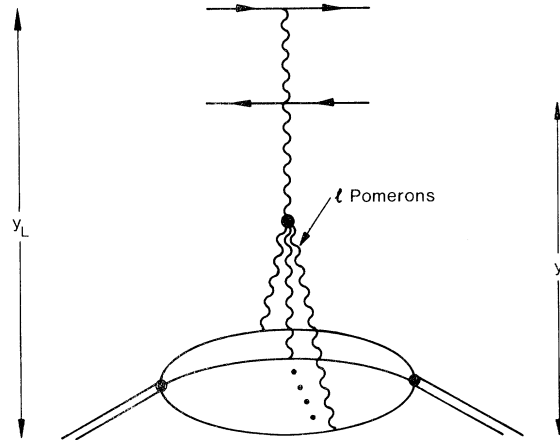


FIG. 14. Production from a general fan diagram.

(3) In the weak-coupling theory of the Pomeron the spectrum  $(1/\sigma_{\text{inel}})(d\sigma/dy)$  for  $y \gtrsim \ln(4R\bar{m})$  is the same for any target.

(4) Elastic scattering is dominated by single- $P$  exchange (see Fig. 9), as is inclusive production.

(5) The absorption length of the  $P$  in nuclear matter might, in principle, permit a distinction between strong- and weak-coupling theories. For this to be accomplished, data at very high energy would be necessary.

(6) The above conclusions (2) and (3) of the weak-coupling theory agree reasonably well with present data from emulsions.

(7) The crucial difference between the present type of model and the "hadronic matter" type models lies in the space-time properties. It is because multiperipheral production takes place over a large region of  $z$  and  $t$  that there is no cascading. A clear test lies in the forward inclusive proton spectrum and its  $A$  dependence.

Whichever way this test goes, it is clear that high-energy scattering from nuclei gives crucial information about the space-time properties of particle production. We can hardly doubt that the same will be true for large- $p_{\perp}$  events and also for high-energy lepton processes.

## ACKNOWLEDGMENT

We thank John Cardy for many interesting discussions about Reggeon calculus.

- <sup>1</sup>This has been especially emphasized by K. Gottfried [CERN Report No. CERN TH 1735, 1973 (unpublished); Phys. Rev. Lett. **32**, 957 (1974)]. See also A. Dar and J. Vary, Phys. Rev. D **6**, 2412 (1972); P. M. Fishbane and J. S. Trefil, Phys. Rev. Lett. **31**, 734 (1973); A. S. Goldhaber, Phys. Rev. D **7**, 765 (1973).
- <sup>2</sup>V. N. Gribov, Yad. Fiz. **9**, 640 (1969) [Sov. J. Nucl. Phys. **9**, 369 (1969)]. See also J. Kogut and L. Susskind, Phys. Rep. **8C**, 78 (1973).
- <sup>3</sup>In this paper the "bare"  $P$  is denoted by a dashed line and the physical  $P$  by a wavy line.
- <sup>4</sup>V. N. Gribov and A. A. Migdal, Yad. Fiz. **8**, 1002 (1968) [Sov. J. Nucl. Phys. **8**, 583 (1969)].
- <sup>5</sup>V. N. Gribov and A. A. Migdal, Zh. Eksp. Teor. Fiz. **55**, 1498 (1968) [Sov. Phys.—JETP **28**, 784 (1969)].
- <sup>6</sup>V. A. Abramovskii, O. V. Kancheli, and V. N. Gribov, in *Proceedings of the XVI International Conference on High Energy Physics, Chicago-Batavia, Ill., 1972*, edited by J. D. Jackson and A. Roberts (NAL, Batavia, Ill., 1973), Vol. 1, p. 389.
- <sup>7</sup>E. Lehman and G. A. Winbow, Daresbury Laboratory Report (in preparation).
- <sup>8</sup>In a previous paper [E. Lehman and G. A. Winbow, Phys. Lett. **48B**, 372 (1973)] we assumed on phenomenological grounds that centrally produced particles could cascade. This assumption is here shown to be wrong.
- <sup>9</sup>J. Cardy and A. R. White, Nucl. Phys. **B80**, 12 (1974).
- <sup>10</sup>J. B. Bronzan, Phys. Rev. D **7**, 480 (1972).
- <sup>11</sup>J. L. Cardy, Nucl. Phys. **B79**, 317 (1974).
- <sup>12</sup>A. A. Migdal *et al.*, Phys. Lett. **48B**, 239 (1974).
- <sup>13</sup>R. J. Glauber, in *High Energy Physics and Nuclear Structure*, edited by G. Alexander (North-Holland, Amsterdam, 1967), p. 311.
- <sup>14</sup>J. V. Allaby *et al.*, Yad. Fiz. **12**, 538 (1970) [Sov. J. Nucl. Phys. **12**, 295 (1971)].
- <sup>15</sup>B. W. Allardyce *et al.*, Nucl. Phys. **A209**, 1 (1973).
- <sup>16</sup>M. Gell-Mann and B. M. Udgaonkar, Phys. Rev. Lett. **8**, 346 (1962).
- <sup>17</sup>H. D. I. Abarbanel and J. B. Bronzan, Phys. Rev. D **9**, 2397 (1974).
- <sup>18</sup>H. D. I. Abarbanel and J. B. Bronzan, Phys. Rev. D **9**, 3304 (1974).
- <sup>19</sup>M. I. Atanelishvili *et al.*, Zh. Eksp. Teor. Fiz. Pis'ma Red. **18**, 490 (1973) [JETP Lett. **18**, 288 (1974)].
- <sup>20</sup>V. V. Ammosov *et al.*, Nucl. Phys. **B58**, 77 (1973).
- <sup>21</sup>Many of the data are discussed and summarized in Ref. 1. See also J. Gierula and W. Wolter, Acta Phys. Pol. **B2**, 95 (1971), and E. L. Feinberg, Phys. Rep. **5C**, 240 (1972), for general discussions of cosmic-ray results.
- <sup>22</sup>Barcelona-Batavia-Belgrade-Bucharest-Lund-Lyons-Montreal-Nancy-Ottawa-Paris-Rome-Strasbourg-Valencia Collaboration (J. Hébert *et al.*), Phys. Lett. **48B**, 467 (1974).
- <sup>23</sup>E. M. Friedlander *et al.*, Nuovo Cimento Lett. **9**, 341 (1974). These data differ from those of J. Babecki *et al.*, Phys. Lett. **47B**, 268 (1973).
- <sup>24</sup>L. D. Landau, Izv. Akad. Nauk SSSR **17**, 51 (1953); S. Z. Belen'kij and L. D. Landau, Nuovo Cimento Suppl. **3**, 15 (1956).
- <sup>25</sup>I. Ya. Pomeranchuk, Dokl. Akad. Nauk SSSR **78**, 889 (1951).
- <sup>26</sup>K. M. Abdo *et al.*, Dubna Report No. DUBNA E1-7548 1973 (unpublished).
- <sup>27</sup>O. V. Kancheli, Zh. Eksp. Teor. Fiz. Pis'ma Red. **18**, 465 (1973) [JETP Lett. **18**, 274 (1973)].

## Unified description of inclusive and exclusive reactions at all momentum transfers\*

R. Blankenbecler and S. J. Brodsky

Stanford Linear Accelerator Center, Stanford University, Stanford, California 94305

(Received 28 May 1974)

The constituent-interchange model is used to relate large- and small-momentum-transfer reactions, to relate inclusive and exclusive processes, and to predict the form of the inclusive cross section throughout the Peyrou plot. Two important corrections to the triple-Regge formula are derived. The first, important at a small missing mass, allows a smooth connection to exclusive processes. The second, important at large missing mass, allows a smooth connection to the central region and to the large-transverse-momentum regime. Simple quark-counting rules are given which predict the limiting behavior of Regge trajectories and residue functions, and also the powers of  $P_T^2$  and the missing-mass dependence of inclusive cross sections. Many experimental consequences of the model are given.

### I. INTRODUCTION

One of the most exciting aspects of large-transverse-momentum hadron reactions is the possibility that we can probe the simplest constituent structure and underlying dynamics of hadronic matter at short distances. Recent data for inclusive and exclusive processes at large  $p_T$  ap-

pear to be consistent with scaling laws of the form<sup>1-4</sup>

$$E \frac{d\sigma}{d^3p} (A+B \rightarrow C+X) - (p_T^2)^{-N} f\left(\frac{\mathfrak{M}^2}{s}, \frac{t}{s}\right)$$

and<sup>5,6</sup>

$$\frac{d\sigma}{dt} (A+B \rightarrow C+D) - (p_T^2)^{-N} f\left(\frac{t}{s}\right)$$